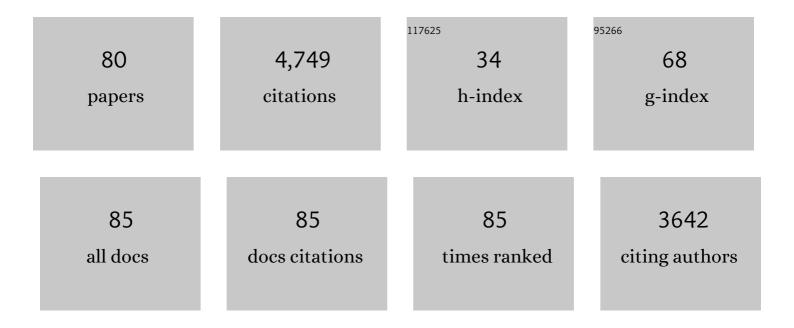
Lianyi Y Chen

List of Publications by Year in descending order

Source: https://exaly.com/author-pdf/8962196/publications.pdf Version: 2024-02-01



#	Article	IF	CITATIONS
1	Uncertainties Induced by Processing Parameter Variation in Selective Laser Melting of Ti6Al4V Revealed by In-Situ X-ray Imaging. Materials, 2022, 15, 530.	2.9	6
2	Effects of Particle Size Distribution with Efficient Packing on Powder Flowability and Selective Laser Melting Process. Materials, 2022, 15, 705.	2.9	7
3	Defects and anomalies in powder bed fusion metal additive manufacturing. Current Opinion in Solid State and Materials Science, 2022, 26, 100974.	11.5	157
4	Revealing melt flow instabilities in laser powder bed fusion additive manufacturing of aluminum alloy via in-situ high-speed X-ray imaging. International Journal of Machine Tools and Manufacture, 2022, 175, 103861.	13.4	26
5	Controlling process instability for defect lean metal additive manufacturing. Nature Communications, 2022, 13, 1079.	12.8	59
6	An instrument for <i>in situ</i> characterization of powder spreading dynamics in powder-bed-based additive manufacturing processes. Review of Scientific Instruments, 2022, 93, 043707.	1.3	5
7	Mitigating keyhole pore formation by nanoparticles during laser powder bed fusion additive manufacturing. Additive Manufacturing Letters, 2022, 3, 100068.	2.1	8
8	In Situ Synchrotron and Neutron Characterization of Additively Manufactured Alloys. Jom, 2021, 73, 174-176.	1.9	2
9	In-Situ Characterization of Pore Formation Dynamics in Pulsed Wave Laser Powder Bed Fusion. Materials, 2021, 14, 2936.	2.9	13
10	Quantitative investigation of gas flow, powder-gas interaction, and powder behavior under different ambient pressure levels in laser powder bed fusion. International Journal of Machine Tools and Manufacture, 2021, 170, 103797.	13.4	21
11	In-situ full-field mapping of melt flow dynamics in laser metal additive manufacturing. Additive Manufacturing, 2020, 31, 100939.	3.0	69
12	<i>In situ</i> / <i>operando</i> synchrotron x-ray studies of metal additive manufacturing. MRS Bulletin, 2020, 45, 927-933.	3.5	22
13	Types of spatter and their features and formation mechanisms in laser powder bed fusion additive manufacturing process. Additive Manufacturing, 2020, 36, 101438.	3.0	48
14	Direct observation of pore formation mechanisms during LPBF additive manufacturing process and high energy density laser welding. International Journal of Machine Tools and Manufacture, 2020, 153, 103555.	13.4	143
15	In situ Characterization of Laser Powder Bed Fusion Using High-Speed Synchrotron X-ray Imaging Technique. Microscopy and Microanalysis, 2019, 25, 2566-2567.	0.4	2
16	Pore elimination mechanisms during 3D printing of metals. Nature Communications, 2019, 10, 3088.	12.8	158
17	Bulk-Explosion-Induced Metal Spattering During Laser Processing. Physical Review X, 2019, 9, .	8.9	34
18	In-situ characterization and quantification of melt pool variation under constant input energy density in laser powder bed fusion additive manufacturing process. Additive Manufacturing, 2019, 28, 600-609.	3.0	103

#	Article	IF	CITATIONS
19	High-speed Synchrotron X-ray Imaging of Laser Powder Bed Fusion Process. Synchrotron Radiation News, 2019, 32, 4-8.	0.8	17
20	Investigating Powder Spreading Dynamics in Additive Manufacturing Processes by <i>In-situ</i> High-speed X-ray Imaging. Synchrotron Radiation News, 2019, 32, 9-13.	0.8	16
21	Transient dynamics of powder spattering in laser powder bed fusion additive manufacturing process revealed by in-situ high-speed high-energy x-ray imaging. Acta Materialia, 2018, 151, 169-180.	7.9	276
22	Revealing particle-scale powder spreading dynamics in powder-bed-based additive manufacturing process by high-speed x-ray imaging. Scientific Reports, 2018, 8, 15079.	3.3	85
23	Ultrafast X-ray imaging of laser–metal additive manufacturing processes. Journal of Synchrotron Radiation, 2018, 25, 1467-1477.	2.4	142
24	Nanoparticle-induced unusual melting and solidification behaviours of metals. Nature Communications, 2017, 8, 14178.	12.8	70
25	Real-time monitoring of laser powder bed fusion process using high-speed X-ray imaging and diffraction. Scientific Reports, 2017, 7, 3602.	3.3	389
26	Phase control in immiscible Zn-Bi alloy by tungsten nanoparticles. Materials Letters, 2016, 174, 213-216.	2.6	23
27	Strengthening Al–Bi–TiCO.7NO.3 nanocomposites by Cu addition and grain refinement. Materials Science & Engineering A: Structural Materials: Properties, Microstructure and Processing, 2016, 651, 332-335.	5.6	17
28	Control of fluid dynamics by nanoparticles in laser melting. Journal of Applied Physics, 2015, 117, 114901.	2.5	9
29	A physically-based plastic constitutive model considering nanoparticle cluster effect for metal matrix nanocomposites. Materials Science & Engineering A: Structural Materials: Properties, Microstructure and Processing, 2015, 641, 172-180.	5.6	12
30	Fabrication of Hierarchical Metallic Nanocomposite Core/Metal Shell Nanostructures by Self-Assembly. Journal of Nanoscience and Nanotechnology, 2015, 15, 5479-5483.	0.9	0
31	Processing and properties of magnesium containing a dense uniform dispersion of nanoparticles. Nature, 2015, 528, 539-543.	27.8	582
32	High Performance Mg6Zn Nanocomposites Fabricated through Friction Stir Processing. , 2015, , 383-386.		2
33	Rapid control of phase growth by nanoparticles. Nature Communications, 2014, 5, 3879.	12.8	116
34	Tuning local structures in metallic glasses by cooling rate. Intermetallics, 2014, 44, 94-100.	3.9	14
35	Facile and scalable synthesis of Ti ₅ Si ₃ nanoparticles in molten salts for metal-matrix nanocomposites. Chemical Communications, 2014, 50, 1454-1457.	4.1	26
36	Urchin-like AlOOH nanostructures on Al microspheres grown via in-situ oxide template. Materials Science and Engineering B: Solid-State Materials for Advanced Technology, 2014, 188, 89-93.	3.5	5

#	Article	IF	CITATIONS
37	Bending behavior of electrodeposited glassy Pd–P and Pd–Ni–P thin films. Scripta Materialia, 2013, 68, 455-458.	5.2	6
38	Achieving uniform distribution and dispersion of a high percentage of nanoparticles in metal matrix nanocomposites by solidification processing. Scripta Materialia, 2013, 69, 634-637.	5.2	106
39	Ultrasonic-Assisted Synthesis of Surface-Clean TiB ₂ Nanoparticles and Their Improved Dispersion and Capture in Al-Matrix Nanocomposites. ACS Applied Materials & Interfaces, 2013, 5, 8813-8819.	8.0	48
40	Effect of fabrication and processing technology on the biodegradability of magnesium nanocomposites. Journal of Biomedical Materials Research - Part B Applied Biomaterials, 2013, 101B, 870-877.	3.4	24
41	Atomic-scale mechanisms of tension–compression asymmetry in a metallic glass. Acta Materialia, 2013, 61, 1843-1850.	7.9	31
42	Assembly of metals and nanoparticles into novel nanocomposite superstructures. Scientific Reports, 2013, 3, .	3.3	38
43	Atomic and cluster level dense packing contributes to the high glass-forming ability in metallic glasses. Intermetallics, 2013, 34, 106-111.	3.9	14
44	Large-scale solution synthesis of α-AlF3·3H2O nanorods under low supersaturation conditions and their conversion to porous β-AlF3 nanorods. Journal of Materials Chemistry, 2012, 22, 20991.	6.7	9
45	Thermal oxidation effect on corrosion behavior of Zr46Cu37.6Ag8.4Al8 bulk metallic glass. Intermetallics, 2012, 22, 84-91.	3.9	12
46	Theoretical study and pathways for nanoparticle capture during solidification of metal melt. Journal of Physics Condensed Matter, 2012, 24, 255304.	1.8	112
47	Atomic-Scale Mechanisms of the Class-Forming Ability in Metallic Glasses. Physical Review Letters, 2012, 109, 105502.	7.8	103
48	Cuï£įZrï£įAlï£įTi Bulk Metallic Glass with Enhanced Glassâ€Forming Ability, Mechanical Properties, Corrosion Resistance and Biocompatibility. Advanced Engineering Materials, 2012, 14, 195-199.	3.5	11
49	Mapping the Strain Distributions in Deformed Bulk Metallic Glasses Using Hard X-Ray Diffraction. Metallurgical and Materials Transactions A: Physical Metallurgy and Materials Science, 2012, 43, 1558-1563.	2.2	11
50	Novel nanoprocessing route for bulk graphene nanoplatelets reinforced metal matrix nanocomposites. Scripta Materialia, 2012, 67, 29-32.	5.2	299
51	Effect of core-shelled nanoparticles of carbon-coated nickel on magnesium. Materials Science & Engineering A: Structural Materials: Properties, Microstructure and Processing, 2012, 546, 284-290.	5.6	12
52	The effect of oxidation on the corrosion resistance and mechanical properties of a Zr-based metallic glass. Corrosion Science, 2011, 53, 3557-3565.	6.6	42
53	Structural origin of the different glass-forming abilities in ZrCu and ZrNi metallic glasses. Journal of Materials Research, 2011, 26, 2098-2102.	2.6	27
54	Mechanical properties of 7–10 mm bone grafts and small slurry grafts in impaction bone grafting. Journal of Orthopaedic Research, 2011, 29, 1491-1495.	2.3	8

#	Article	IF	CITATIONS
55	A plastic Zr–Cu–Ag–Al bulk metallic glass. Acta Materialia, 2011, 59, 1037-1047.	7.9	55
56	Atomic structure in Al-doped multicomponent bulk metallic glass. Scripta Materialia, 2010, 63, 879-882.	5.2	39
57	"Soft―atoms in Zr70Pd30 metal–metal amorphous alloy. Scripta Materialia, 2010, 63, 883-886.	5.2	7
58	Effect of pre-existing shear bands on the tensile mechanical properties of a bulk metallic glass. Acta Materialia, 2010, 58, 1276-1292.	7.9	117
59	Shear band evolution and hardness change in cold-rolled bulk metallic glasses. Acta Materialia, 2010, 58, 4827-4840.	7.9	95
60	Reply to the comments of Y.H. Liu: Ion sputter erosion in metallic glass—A response to "Comment on: Homogeneity of Zr64.13Cu15.75Ni10.12Al10 bulk metallic glass―by L-Y. Chen, Y-W. Zeng, Q-P. Cao, B-J. Park, Y-M. Chen, K. Hono, U. Vainio, Z-L. Zhang, U. Kaiser, X-D. Wang,and J-Z Jiang [J. Mater. Res. 24, 3116 (2009)]. Journal of Materials Research, 2010, 25, 602-604.	2.6	4
61	Structural origin of the high glass-forming ability in Y-doped bulk metallic glasses. Journal of Materials Research, 2010, 25, 1701-1705.	2.6	13
62	Initiation and evolution of shear bands in bulk metallic glass under tension—An in situ scanning electron microscopy observation. Journal of Materials Research, 2009, 24, 2924-2930.	2.6	1
63	Homogeneity of the superplastic Zr _{64.13} Cu _{15.75} Ni _{10.12} Al ₁₀ bulk metallic glass. Journal of Materials Research, 2009, 24, 3116-3120.	2.6	11
64	Catching Fe-based bulk metallic glass with combination of high glass forming ability, ultrahigh strength and good plasticity in Fe–Co–Nb–B system. Materials Science & Engineering A: Structural Materials: Properties, Microstructure and Processing, 2009, 517, 246-248.	5.6	36
65	Effect of microalloying of Nb on corrosion resistance and thermal stability of ZrCu-based bulk metallic glasses. Journal of Non-Crystalline Solids, 2009, 355, 203-207.	3.1	27
66	Wear behavior of a series of Zr-based bulk metallic glasses. Materials Science & Engineering A: Structural Materials: Properties, Microstructure and Processing, 2008, 475, 124-127.	5.6	29
67	Free-volume-induced enhancement of plasticity in a monolithic bulk metallic glass at room temperature. Scripta Materialia, 2008, 59, 75-78.	5.2	116
68	Stress-induced softening and hardening in a bulk metallic glass. Scripta Materialia, 2008, 59, 1210-1213.	5.2	40
69	Formation of Ni–Nb–Zr–X (X = Ti, Ta, Fe, Cu, Co) bulk metallic glasses. Journal of Alloys and Compounds, 2008, 460, 714-718.	5.5	30
70	Achieving large macroscopic compressive plastic deformation and work-hardening-like behavior in a monolithic bulk metallic glass by tailoring stress distribution. Applied Physics Letters, 2008, 92, .	3.3	40
71	New Class of Plastic Bulk Metallic Glass. Physical Review Letters, 2008, 100, 075501.	7.8	182
72	Tension and stress relaxation behavior of a La-based bulk metallic glass. Journal of Materials Research, 2007, 22, 3303-3308.	2.6	3

#	Article	IF	CITATIONS
73	Ultrahigh strength binary Ni–Nb bulk glassy alloy composite with good ductility. Journal of Alloys and Compounds, 2007, 443, 105-108.	5.5	23
74	Catching the Ni-based ternary metallic glasses with critical diameter up to 3mm in Ni–Nb–Zr system. Journal of Alloys and Compounds, 2007, 443, 109-113.	5.5	52
75	Formation of bulk metallic glasses in Cu45Zr48â^'xAl7REx (RE=La, Ce, Nd, Gd and 0≤â‰\$at.%). Intermetallics, 2007, 15, 1066-1070.	3.9	26
76	Ultrasonic-assisted preparation of monodisperse iron oxide nanoparticles. Materials Letters, 2007, 61, 2204-2207.	2.6	17
77	Design of Cu8Zr5-based bulk metallic glasses. Applied Physics Letters, 2006, 88, 241913.	3.3	67
78	Synthesis of centimeter-size Ag-doped Zr–Cu–Al metallic glasses with large plasticity. Journal of Alloys and Compounds, 2006, 424, 176-178.	5.5	51
79	Centimeter-sized (La0.5Ce0.5)-based bulk metallic glasses. Journal of Alloys and Compounds, 2006, 424, 179-182.	5.5	20
80	Glass formability, thermal stability and mechanical properties of La-based bulk metallic glasses. Journal of Alloys and Compounds, 2006, 424, 183-186.	5.5	48